Fuel Communications 10 (2022) 100049

Contents lists available at ScienceDirect

Fuel Communications

journal homepage: www.sciencedirect.com/journal/fuel-communications

Challenges in Kinetic modeling of ammonia pyrolysis

Peter Glarborg [*,a], Hamid Hashemi [a], Paul Marshall [b]

[a] Department of Chemical and Biochemical Engineering, Technical University of Denmark, Kgs. Lyngby DK-2800, Denmark
[b] Department of Chemistry and Center for Advanced Scientific Computing and Modeling, University of North Texas, 1155 Union Circle #305070, Denton, Texas 76203-5017, USA

A B S T R A C T

Ammonia pyrolysis reactions have implications for its ignition and oxidation in engines and gas turbines. In the present work, the chemistry of ammonia pyrolysis is investigated by kinetic modeling and theory. Rate constants for key reactions are carefully evaluated based on available experimental and theoretical results. The high pressure limit $k_{1,\infty}$ for $NH_2 + H$ (+M) ⇄ NH_3 (+M) (R1) is calculated to be essentially the collision frequency, indicating that dissociation of ammonia in combustion processes will be at or close to the low pressure limit even at engine and gas turbine conditions. The chemical kinetic model is validated against reported shock tube measurements of NH_3, NH_2, and NH in ammonia pyrolysis. Predictions are in good agreement with observations for dilute conditions ($\leq$ 0.5% NH_3), but the model appears to underpredict the NH_3 consumption rate at longer times in less dilute mixtures. At short reaction times, thermal dissociation of NH_3, together with the $NH_3 + H$ reaction, controls conversion. At longer times, secondary reactions involving NH_2 and NH become important due to their impact on the radical pool. Predictions become sensitive to formation and consumption of diazene (tHNNH and cHNNH). Several of the key steps in the ammonia pyrolysis mechanism are radical-radical reactions that are difficult to measure accurately and challenging to calculate theoretically, and a more comprehensive experimental characterization is desirable to support further model development.

1. Introduction

The potential of ammonia as a carbon-free energy carrier is currently investigated extensively [1–4]. Contrary to combustion of nitrogen-containing fossil fuels [5,6], the application of ammonia as the main fuel in engines or gas turbines involves conditions with high concentrations of NH_3 and high pressure. The ignition delay time, flame speed, and the ammonia consumption rate, particularly in local fuel-rich areas, are sensitive to reactions in ammonia pyrolysis. These include thermal dissociation,

$$NH_3(+M) \rightleftarrows NH_2 + H(+M), (R1b)$$

reactions of amines with H, e.g.,

$$NH_3 + H \rightleftarrows NH_2 + H_2 (R2)$$

$$NH_2 + H \rightleftarrows NH + H_2, (R4)$$

and amine-amine steps such as

$$NH_2 + NH_2 \rightleftarrows NH_3 + NH (R5)$$

$$NH_2 + NH_2(+M) \rightleftarrows N_2H_4(+M) (R8)$$

$$NH_2 + NH \rightleftarrows HNNH + H (R9, R10)$$

The reaction numbering refers to Table 2 below.

Decomposition of ammonia has been studied in shock tubes [7–17], flow reactors [18,19], jet-stirred reactors [20], and static reactors [21]. Konnov and De Ruyck [22] developed a detailed reaction mechanism for ammonia pyrolysis and validated it by comparison to shock tube results from Davidson et al. [15]. They emphasized the importance of taking into account the N_2-amine chemistry in the interpretation of ammonia pyrolysis data and proposed a reaction between NH_3 and NH_2 to form N_2H_3 as important.

Since the work of Konnov and De Ruyck [22], a number of studies of relevance to ammonia pyrolysis chemistry have been published. Recent experimental work have been conducted in flow reactors [19], jet-stirred reactors [20], and shock tubes [17]. Notably, Alturaifi et al. [17] conducted an experimental and modeling study of ammonia pyrolysis in a shock tube, measuring NH_3 concentration profiles under dilute, near-atmospheric pressure conditions in the temperature range 2100-3000 K. Based on their results, as well as data from literature, they revised the ammonia pyrolysis mechanism, improving predictions compared to literature mechanisms.

Also a number of theoretical studies have served to improve our understanding of the amine pyrolysis chemistry. Bugler et al. [23] used

* Corresponding author.
E-mail address: pgl@kt.dtu.dk (P. Glarborg).

https://doi.org/10.1016/j.jfueco.2022.100049
Received 27 October 2021; Received in revised form 8 January 2022; Accepted 10 January 2022
Available online 12 January 2022

Table 1
Heats of formation (298 K) for selected amine species. Units are kcal mol^{-1}.

Species	NH_3	NH_2	NH	N_2H_4	N_2H_3	tHNNH	cHNNH	H_2NN
Bugler et al. [23]	-10.43	44.58	85.10	23.94	53.91	48.59	53.79	72.39
Present work	-10.89[a]	44.45[a]	85.74[a]	23.20[b]	53.73[c]	47.78[d]	52.97[d]	71.92[e]

[a] Glarborg et al. [6];
[b] Dorofeeva et al. [32] and Feller et al. [30];
[c] Active Thermochemical Tables (ATcT) [31];
[d] Marshall et al. [28];
[e] Burcat database [29].

Table 2
Selected reactions in the ammonia pyrolysis subset. Parameters for use in the modified Arrhenius expression $k = AT^{\beta} \exp(-E/[RT])$. Units are mol, cm, s, cal.

		A	β	E_a	Source
1.	$NH_2 + H(+M) \rightleftarrows NH_3(+M)$	1.5E14	0.167	0	See text
	Low pressure limit (Ar)	3.0E22	-1.900	0	
	Low pressure limit (N_2)	2.6E23	-2.083	0	
	Troe parameters: 0.5 1E-30 1E30 1E30				
	Collision efficiencies[a] (Ar/N_2): $NH_3 = 20/9$				[27]
2.	$NH_3 + H \rightleftarrows NH_2 + H_2$	5.4E05	2.400	9916	[33]
3.	$NH + H + M \rightleftarrows NH_2 + M$	1.2E25	-2.710	0	[34], rv
4.	$NH_2 + H \rightleftarrows NH + H_2$	5.1E08	1.500	3700	See text
5.	$NH_2 + NH_2 \rightleftarrows NH_3 + NH$	5.6E00	3.530	552	[24]
6.	$NH_2 + NH_2 \rightleftarrows tHNNH + H_2$	1.7E08	1.020	11783	[24]
7.	$NH_2 + NH_2 \rightleftarrows H_2NN + H_2$	7.2E04	1.880	8802	[24]
8.	$NH_2 + NH_2(+M) \rightleftarrows N_2H_4(+M)$	5.6E14	-0.414	66	[24]
	Low pressure limit:	1.6E34	-5.490	1987	
9.	$NH_2 + NH \rightleftarrows tHNNH + H$	1.2E15	-0.500	0	[15,28]
10.	$NH_2 + NH \rightleftarrows cHNNH + H$	3.0E14	-0.500	0	[15,28]
11.	$NH_2 + NH \rightleftarrows NH_3 + N$	9.6E03	2.460	107	[24]
12.	$NH_2 + N \rightleftarrows N_2 + H + H$	7.0E13	0.000	0	[35]
13.	$NH + M \rightleftarrows N + H + M$	1.8E14	0.000	74800	[34]
14.	$NH + H \rightleftarrows N + H_2$	3.5E13	0.000	0	[36,37]
15.	$NH + NH \rightleftarrows NNH + H$	6.2E13	-0.036	-161	[24]
16.	$tHNNH(+M) \rightleftarrows cHNNH(+M)$	4.9E09	1.180	47700	[28]
	Low pressure limit:	3.0E28	-3.560	56100	
	Troe parameters: 0.35 650 10600				
	$tHNNH(+M) \rightleftarrows cHNNH(+M)$	1.5E14	0.000	55000	
	Low pressure limit:	2.3E29	-4.000	60100	
	Troe parameters: 0.35 650 10600				
	Duplicate reaction				
17.	$tHNNH(+M) \rightleftarrows NNH + H(+M)$	6.3E16	0.000	63980	[28]
	Low pressure limit:	8.7E39	-6.910	70400	
	Troe parameters: 0.44 520 6150				
18.	$cHNNH(+M) \rightleftarrows NNH + H(+M)$	5.7E16	0.000	58600	[28]
	Low pressure limit:	9.6E35	-5.440	63980	
	Troe parameters: 0.44 520 6150				
19.	$tHNNH + H \rightleftarrows NNH + H_2$	9.6E07	1.800	900	[28]
20.	$tHNNH + NH_2 \rightleftarrows NNH + NH0_3$	2.7E05	2.226	-1034	[26]
21.	$cHNNH + H \rightleftarrows NNH + H_2$	2.8E08	1.720	470	[28]
22.	$cHNNH + H \rightleftarrows tHNNH + H$	7.8E08	1.580	2180	[28], low pressure limit

[a] Collision efficiencies (Ar/N_2): $O_2 = 1.5/0.65$, $CH_4 = 13.5/5.9$, $CO_2 = 13/5.6$

quantum chemical composite methods to obtain thermodynamic properties for a range of nitrogen-containing species, while Glarborg et al. [6] reviewed the amine thermochemistry using the Active Thermochemical Tables (ATcT) approach. Klippenstein et al. [24] calculated rate constants for reactions on the N_2H_4 and N_2H_3 potential energy surfaces, including $NH_2 + NH_2$ (R5-R8) and $NH_2 + NH$ (R9, R10). Also Li and Sarathy [25] and Dievart and Catoire [26] have calculated rate constants for reactions important in pyrolysis of amines. Recently, Glarborg et al. [27] calculated collision efficiencies for selected molecules in recombination of NH_2 with H (R1) and NH_2 (R8), and Marshall et al. [28] reported a theoretical study of reactions important for forming or consuming diazene (tHNNH and cHNNH).

Due to the importance of the NH_3 pyrolysis for ignition and oxidation of ammonia in high concentration, it is of interest to once again revisit this chemistry, particularly in light of the recent theoretical work, e.g., [24–28]. In the present study, the pyrolysis mechanism for NH_3 is carefully revised, based on theory as well as re-interpretation of selected experimental data from literature. The pressure dependence of thermal dissociation of NH_3 is investigated and predictions with the updated pyrolysis model is compared to shock tube results from literature.

Chemical Kinetic model

The chemical kinetic model, including rate coefficients and thermodynamic data, was based mainly on the review of nitrogen chemistry by Glarborg et al. [6]. For a number of reactions, rate constants were updated, based on a review of available data or on re-interpretation of shock tube results from literature.

The thermodynamic data are a key component in the kinetic model. There has been some ambiguity in the properties for key amine species, but recent work by Bugler et al. [23] and by Ruscic and coworkers [6, 29–31] have served to reduce the uncertainty. In their modeling study, Alturaifi et al. [17] adopted the thermodynamic properties for the amine species from Bugler et al., while in the present work we rely mostly on data reported by Ruscic and coworkers. Table 1 compares the heats of formation for the key amine species reported by Bugler et al. with those employed in the present work. The differences are all below 1 kcal mol^{-1} and mostly the agreement is within 0.5 kcal mol^{-1}. However, for the present purposes it is a concern with differences of around 0.5 kcal mol^{-1} in $H_{f,298}$ for both NH_3 and NH. Differences of this magnitude are significant when calculating reverse rate constants using the equilibrium constant. In ATcT, $H_{f,298}(NH_3)$ has an estimated uncertainty of less than 0.01 kcal mol^{-1} and the value calculated by Bugler et al. appears to be in error. Results discussed below for the reactions $NH_3 + H \rightleftarrows NH_2 + H_2$, $NH_2 + H \rightleftarrows NH + H_2$, and $NH_3 + NH \rightleftarrows NH_2 + NH_2$ show consistency between measurements of forward and reverse rate constants, supporting the present thermodynamic data, but more work is required to resolve this issue.

Table 2 lists selected reactions in the ammonia pyrolysis subset. The key reaction in pyrolysis of ammonia is its thermal dissociation,

$$NH_3(+M) \rightleftarrows NH_2 + H(+M) \quad (R1b)$$

In the model, we prefer to represent this reaction, as well as a number of other steps, in the exothermic direction, i.e.,

$$NH_2 + H(+M) \rightleftarrows NH_3(+M) \quad (R1)$$

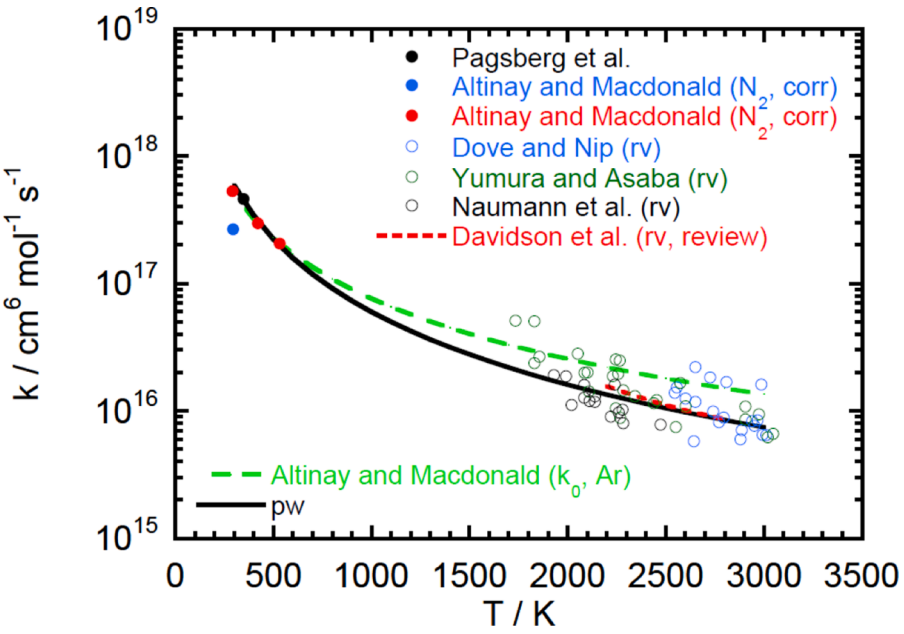

Fig. 1. Data for the low pressure limit $k_{1,0}$ of the $NH_2 + H (+Ar) = NH_3 (+Ar)$ reaction (R1). Symbols denote the experimental data of Pagsberg et al. [38] and Altinay and Macdonald [39,40] for the forward reaction, and data derived from low-pressure measurements of the reverse rate constant by Dove and Nip [11], Yumura and Asaba [13], Naumann et al. [16], and Davidson et al. [15], converted through the equilibrium constant. The data of Altinay and Macdonald were obtained for N_2 as collision partner and have been corrected as discussed in the text. The dashed lines show the rate constants recommended by Altinay and Macdonald [40] and by Davidson et al. [15], while the fit to $k_{1,0}$, obtained in the present work is shown as a solid line.

Data for the low pressure limit have been reported for low temperature in the forward direction ($k_{1,0}$) by Pagsberg et al. [38] and Altinay and Macdonald [39,40], and for high temperature in the reverse direction ($k_{1b,0}$) by Dove and Nip [11], Yumura and Asaba [13], Naumann et al. [16], and Davidson et al. [15]. In their evaluation, Baulch et al. [41] considered the data from Naumann et al. [16] to be the most reliable. Figure 1 compares the experimental data reported at or close to the low pressure limit. Data for the thermal dissociation of NH_3 (R1b) were converted through the equilibrium constant. Most of the data were obtained with Ar as inert gas. The results of Altinay and Macdonald [40] were obtained for N_2 as collision partner; these data were corrected for the difference in third body efficiency (TBE) based on the results of Glarborg et al. [27], roughly represented as $TBE(Ar)/TBE(N_2) = 0.114 \cdot T^{0.183}$.

Our preferred low pressure limit rate constant for $NH_2 + H + Ar$ is based on the low temperature data of Altinay and Macdonald [40] and Pagsberg et al. [38], and the high temperature results from Naumann et al. [16] and Davidson et al.[15]. The evaluation by Davidson et al. [15] was based on re-interpretation of shock tube results from Roose (not published), Dove and Nip [11], Yumura and Asaba [13], and Holzrichter and Wagner [14].

Experimental results for NH_3 dissociation at high pressure are scarce and in poor agreement. Holzrichter and Wagner [14] and Genich et al. [10] have reported data for k_{1b} at elevated pressure from shock tube experiments. Genich et al. conducted experiments at pressures up to 300 atm. Their reported fall-off behavior indicates a high pressure limit $k_{1,\infty}$ of around $2 \cdot 10^{12}$ s^{-1} at 2200-2500 K, with an uncertainty of a factor of five. Holzrichter and Wagner operated at temperatures of 2200-3300 K and at densities up to $2 \cdot 10^{-4}$ mol cm^{-3}, observing fall-off behavior at the highest pressures. Based on the results of Holzrichter and Wagner,

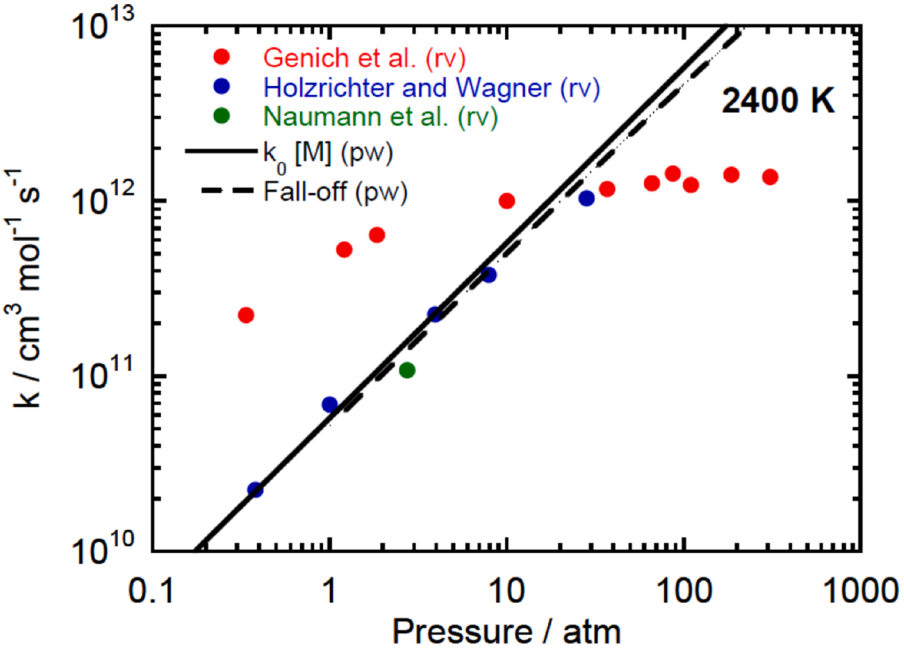

Fig. 2. Fall-off behavior for $NH_2 + H (+Ar) = NH_3 (+Ar)$ (R1) at 2400 K. Symbols denote the experimental data of Genich et al. [10], Holzrichter and Wagner [14], and Naumann et al. [16]. The data from Holzrichter and Wagner have been reduced by a factor 1.7, following the analysis of Davidson et al. [15]. All data are converted through the equilibrium constant. The solid line shows the recommended low pressure limit, while the dashed line denotes the predicted fall-off behavior with the present rate coefficients.

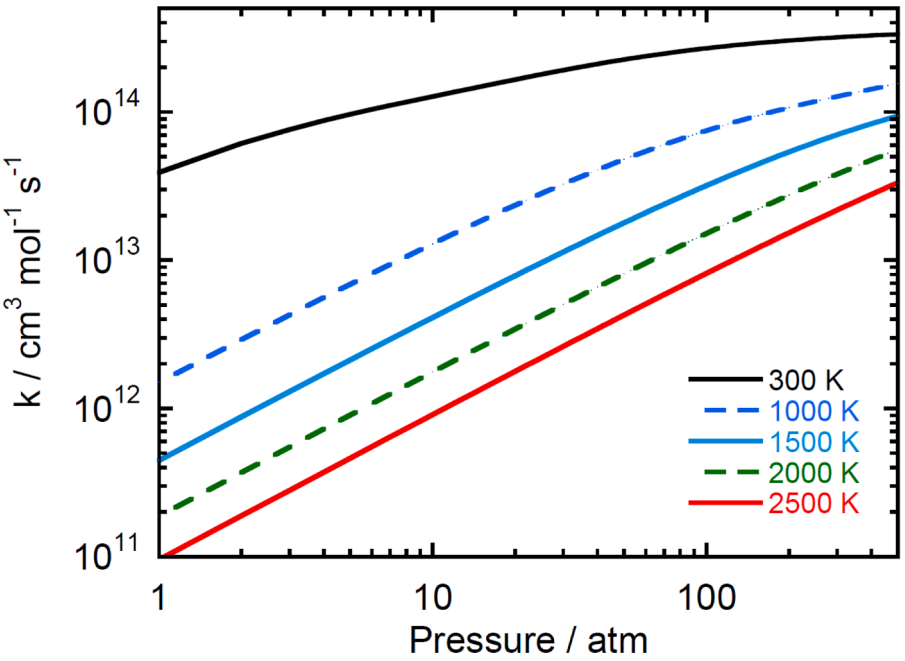

Fig. 3. Predicted fall-off behavior for $NH_2 + H (+N_2) = NH_3 (+N_2)$ (R1) at selected temperatures.

Baulch et al. [41] estimated a high pressure limit for R1b, corresponding to $k_{1,\infty} = 2{\cdot}10^{14}$ s^{-1} at 2000-3000 K, with a significant uncertainty. This value agrees well with the estimate of $k_{1,\infty} = 1.6{\cdot}10^{14}$ s^{-1} chosen by Altinay and Macdonald [40]. They characterized experimentally the fall-off behavior of $NH_2 + H$ (+M) at temperatures of 292-533 K and pressures from a few torr up to 400 torr. They could not derive the high pressure limit based on their experiments, but chose the value of $k_{1,\infty}$ as the basis for their data fitting.

Due to the uncertainty about the high pressure limit for R1, we studied it theoretically. Geometry changes along a relaxed scan of one N-H bond length r in NH_3 from $1.0{\cdot}10^{-10}$ m to $4.0{\cdot}10^{-10}$ m were calculated with the B2PLYP-D3 density functional and the cc-pVTZ basis set using the Gaussian 16 program [42]. Energies were calculated with multi-reference CASSCF-MP2 theory including all configurations of the 8 valence electrons among the 7 molecular orbitals arising from the valence orbitals, relative to the energy at a separation of $r = 5.0{\cdot}10^{-10}$ m. No barrier to $H + NH_2$ addition was found. Accordingly, recombination was evaluated via classical capture theory [43], based on the idea that reactive collisions occur on an attractive potential of the form $V = -C_6/r$ when centrifugal barriers are overcome. The C_6 parameter reflects long-range forces arising mainly from dispersion interactions with a ca. 10% contribution here from dipole-induced dipole interactions. Experimental, if available, or computed data for polarizabilities, ionization

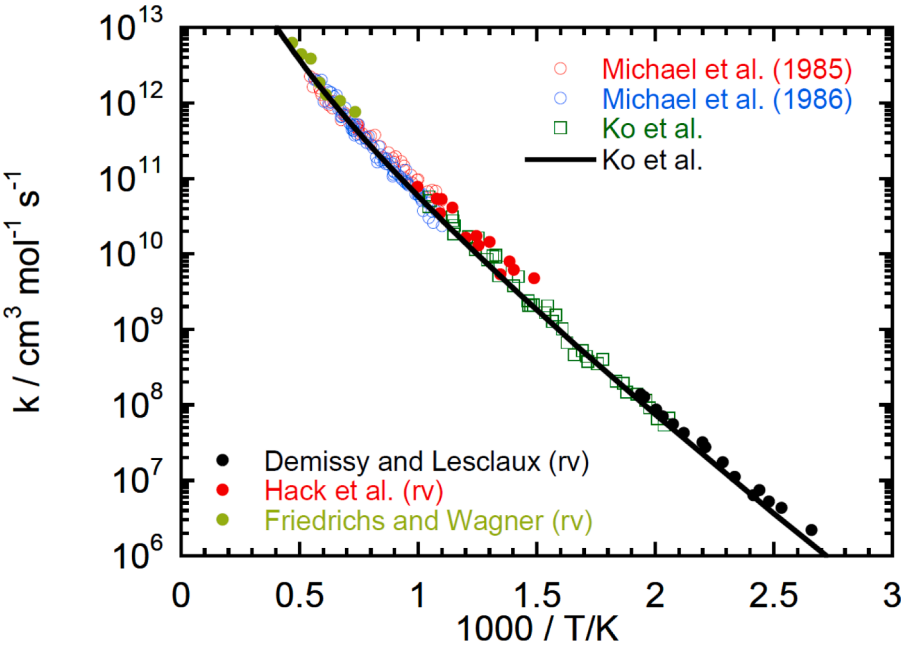

Fig. 4. Arrhenius plot for the reaction $NH_3 + H = NH_2 + H_2$ (R2). Symbols denote the experimental data of Michael et al. [47,48] and Ko et al. [33] for the forward reaction, and data derived from measurements of the reverse rate constant by Demissy and Lesclaux [50], Hack et al. [51], and Friedrichs and Wagner [52], converted through the equilibrium constant. The solid line shows the rate constant recommended by Ko et al.

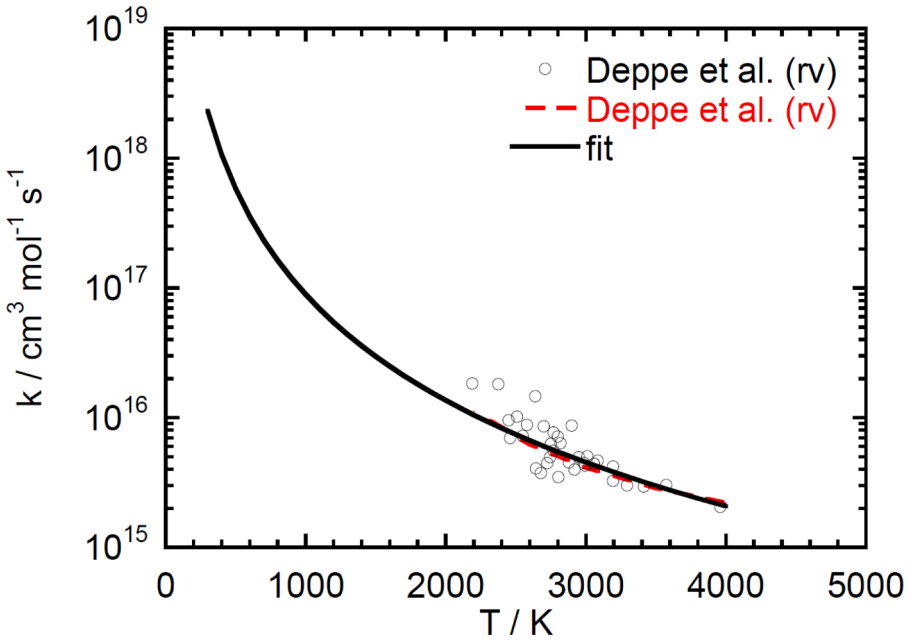

Fig. 5. Arrhenius plot for the reaction NH + H + M = NH_2 + M (R3). Symbols denote data derived from measurements of the reverse rate constant by Deppe et al. [34]. The lines denote best fit rate constants, from the expression of the reverse reaction of Deppe et al., as well as the present fit.

potentials and the NH_2 dipole moment were taken from the NIST compilation [44], which lead to $C_6 \approx 2.0 \cdot 10^{-78}$ J m^6. The high-pressure rate coefficient for recombination, taken to occur at every reactive collision with neglect of recrossing, of $k_{1,\infty} \approx 6.5 \cdot 10^{14}$ cm^3 mol^{-1} s^{-1} at 298 K, proportional to $T^{1/6}$, is derived [43]. The high average velocity of H atoms helps make this significantly larger than a typical hard-sphere collision rate coefficient. Within likely uncertainties, this value and its temperature-dependence are comparable to the ca. $2 \cdot 10^{14}$ cm^3 mol^{-1} s^{-1} recommended for the analogous H + CH_3 recombination at 298 K [45] and to the estimates of the high pressure limit by Baulch et al. [41] and Altinay and Macdonald [40]. Our best estimate is $k_{1,\infty} \approx (4 \pm 2) \cdot 10^{14}$ cm^3 mol^{-1} s^{-1} at room temperature. Should future experimental conditions approach the high-pressure region of H + NH_2, then a more detailed evaluation of $k_{1,\infty}$ would be warranted.

Figure 2 compares the results of Genich et al. [10] with those of Holzrichter and Wagner [14] and Naumann et al. [16] at 2400 K. The low-pressure limit and the predicted fall-off behavior based on the present rate coefficients are also shown. The data of Genich et al. are in poor agreement with the other measurements at overlapping pressures, indicating that they may have faced some experimental difficulties. The data from Holzrichter and Wagner, after making the correction suggested by Davidson et al. [15], are in good agreement with the value reported by Naumann et al. and with the low pressure limit proposed in the present work. The data of Holzrichter and Wagner indicate departure from the low pressure limit at 20-30 atm at this temperature.

Figure 3 compares the predicted fall-off behavior for NH_2 + H (+M) (R1) over a wide temperature and pressure range for N_2 as collision

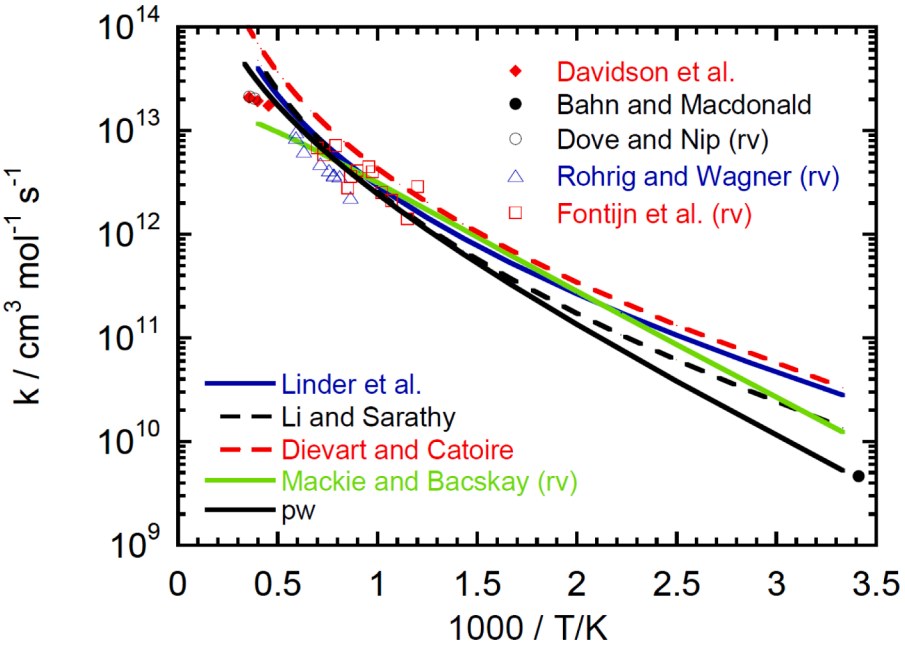

Fig. 6. Arrhenius plot for the reaction NH_2 + H = NH + H_2 (R4). Symbols denote the experimental data of Davidson et al. [15] and Bahn and Macdonald [55] for the forward reaction, and data derived from measurements of the reverse rate constant by Dove and Nip [11], Rohrig and Wagner [56], and Fontijn et al. [57], converted through the equilibrium constant. The lines denote the calculated rate constants by Linder et al. [58], Li and Sarathy [25], Dievart and Catoire [26], and Mackie and Bacskay [59] (from the reverse rate constant), as well as the value used in the present work.

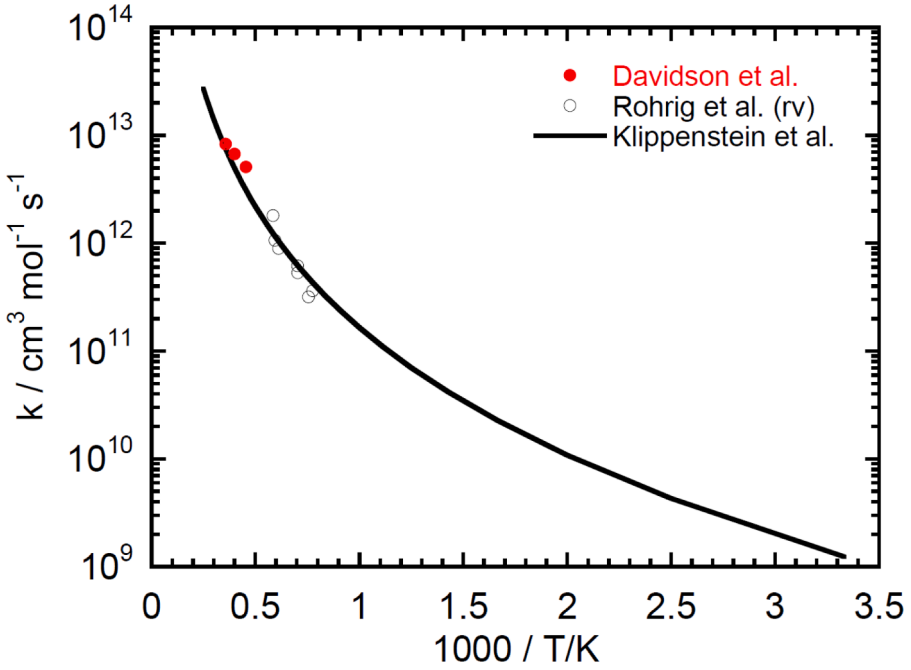

Fig. 7. Arrhenius plot for the reaction $NH_2 + NH_2 = NH_3 + NH$ (R5). Symbols denote the experimental data of Davidson et al. [15] and Rohrig et al. [60]; the latter converted through the equilibrium constant. The solid line denotes the calculated rate constant by Klippenstein et al. [24].

partner. Even under conditions of interest for engines and gas turbines, i.e., high temperature and high pressure, the reaction is at or very close to the low pressure limit. Modeling predictions are not very sensitive to the assumed high pressure limit as long as it is close to the collision frequency.

The reaction of NH_3 with H,

$$NH_3 + H \rightleftarrows NH_2 + H_2 (R2)$$

has been studied extensively over a wide temperature range, both in the forward and reverse direction. Figure 4 shows an Arrhenius plot for the reaction. Results for the forward reaction have been reported by Dove and Nip [46], Michael et al. [47,48], and and Ko et al. [33], which updates Marshall et al. [49]. The reverse reaction was studied by Demissy and Lesclaux [50], Hack et al. [51], and Friedrichs and Wagner [52]. We have omitted the data from Dove and Nip [46], as their measurements show only small sensitivity to k_2. The other results are in good agreement. We have adopted the rate constant proposed by Ko et al. [33].

In addition to NH_3 + H (R2), ammonia could react with amine radicals, primarily NH_2 and NH. The $NH_3 + NH_2$ reaction to form N_2H_3

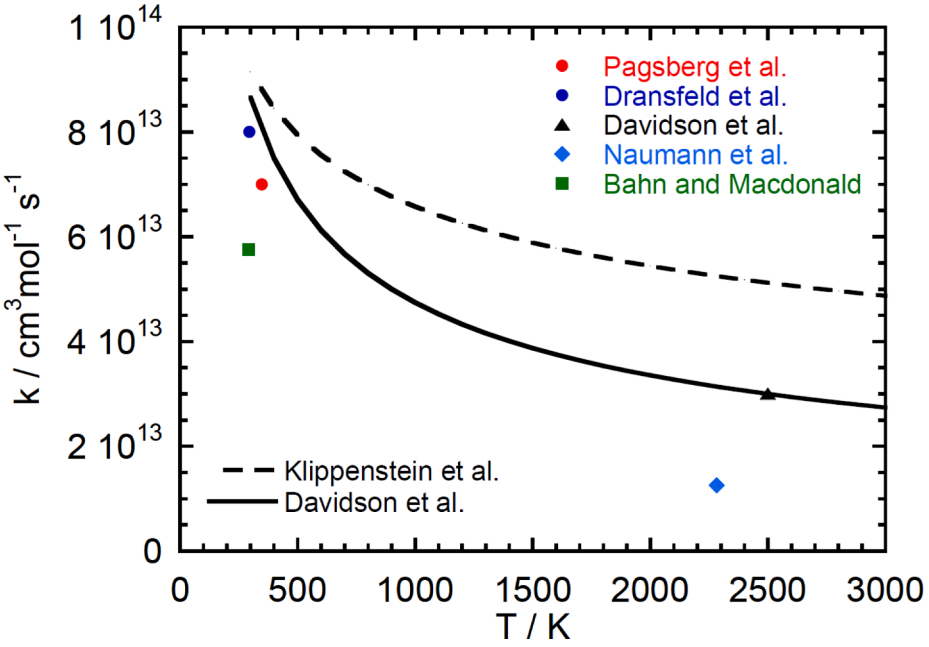

Fig. 8. Rate constant plot for the reaction $NH_2 + NH = HNNH + H$ (R9, R10). Symbols denote the experimental data of Pagsberg et al. [38], Dransfeld et al. [61], Davidson et al. [15], Naumann et al. [16], and Bahn and Macdonald [55]. The dashed line denotes the rate constant calculated by Klippenstein et al. [24], while the solid line shows the evaluation of Davidson et al. [15].

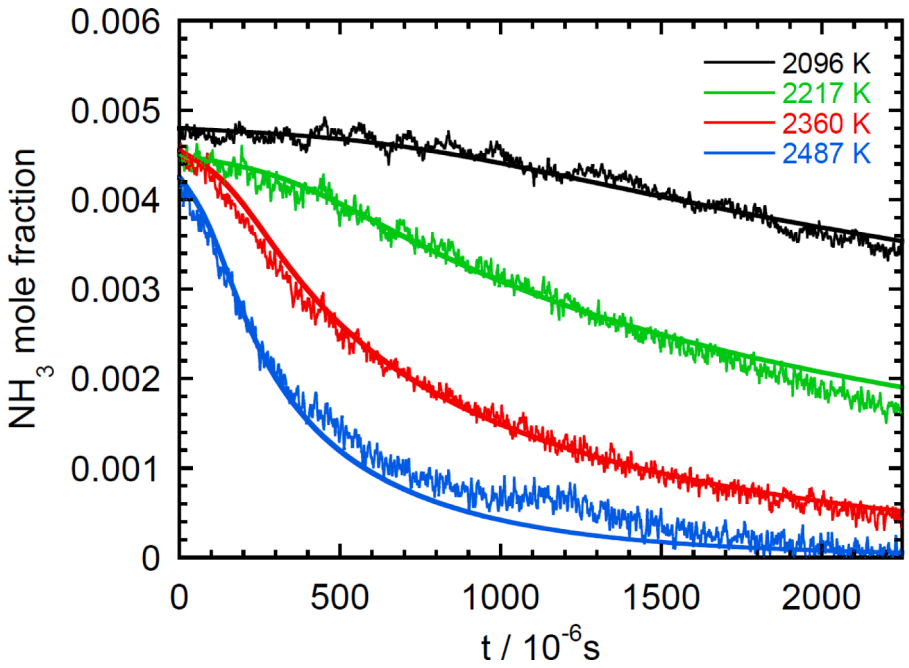

Fig. 9. Comparison of the shock tube measurements of NH_3 by Alturaifi et al. [17] with modeling predictions in decomposition of ammonia. Experimental conditions: about 0.5% NH_3 in Ar at 2096 K (1.25 atm), 2217 K (1.22 atm), 2360 K (1.18 K), and 2487 K (1.12 atm).

$+ H_2$ proposed by Konnov and De Ruyck [22] is currently not supported by any direct experiments or by theory and has been disregarded in the present work. The reaction with NH, the reverse of reaction (R5), is discussed in more detail below.

The NH_2 radical may dissociate at high temperature or react with other radicals. For the thermal dissociation (R3b), we rely on the data from Deppe et al. [34], which constitute the only direct measurements. Figure 5 compares the data, reversed through the equilibrium constant, with the rate constant proposed in the present work. The extrapolation to low temperatures is uncertain, but the reaction is only important at very high temperatures. The present rate constant, $k_3 = 1.2{\cdot}10^{25}\ T^{-2.71}$ $cm^3\ mol^{-1}\ s^{-1}$, is significantly larger than the estimate by Miller and Bowman [53], but in reasonable agreement at high temperature with the value proposed by Hanson and Salimian [54].

In the shock tube experiments of interest in the present work, NH_2 is mainly consumed by reaction with H or NH. The reaction with atomic hydrogen,

$$NH_2 + H \rightleftarrows NH + H_2 (R4)$$

has mostly been studied at high temperature. The Arrhenius plot shown in Fig. 6 includes data obtained for the forward step by Bahn and Macdonald [55] and Davidson et al. [15], and data derived from measurements of the reverse rate constant by Dove and Nip [11], Rohrig and Wagner [56], and Fontijn et al. [57], converted through the equilibrium constant. The rate constant for R4 is difficult to determine because of the impact of side reactions, and possibly the data for R4b are more accurate. The results from Rohrig and Wagner and Fontijn et al. agree within the scatter. The theoretical studies of Linder et al. [58], Li and Sarathy [25] and Dievart and Catoire [26] for R4 and of Mackie and Bacskay [59] for R4b are all in reasonable agreement with the measurements of Rohrig and Wagner and Fontijn et al., but deviate at high temperature from the measurements of Davidson et al. [15] and Dove and Nip [11]. We have tentatively derived a rate constant based on the results reported by Bahn and Macdonald, Rohrig and Wagner, and Fontijn et al., but more work on this reaction is desirable.

The $NH_2 + NH_2$ reaction has several product channels, including formation of N_2 amines (R6, R7). However, under the high temperature conditions investigated in the present work, only disproportionation is important:

$$NH_2 + NH_2 \rightleftarrows NH_3 + NH (R5)$$

High temperature measurements have been conducted in shock tubes for both the forward [15] and the reverse [60] step. We have adopted the rate constant calculated by Klippenstein et al. [24], which is in good agreement with the high temperature results (Fig. 7) and also comply reasonably with the low temperature upper limit reported by Dransfeld et al. [61].

There are only few data available for the reaction,

$$NH_2 + NH \rightleftarrows HNNH + H, (R9, R10)$$

all from indirect measurements. The low temperature results by Pagsberg et al. [38], Dransfeld et al. [61], and Bahn and Macdonald [55], together with the the shock tube data of Davidson et al. [15] and Naumann et al. [16], indicate a fast reaction with a slight negative temperature dependency, in line with expectations for a radical-radical reaction. It is a challenging reaction to characterize experimentally. However, the modeling presented in the present work indicates that the rate constant calculated by Klippenstein et al. [24] may be too fast, and for now we have adopted the value proposed by Davidson et al. [15], based on the available measurements. The branching ratio between the trans and cis isomers of HNNH was adopted from Marshall et al. [28].

Under the conditions evaluated in the present work, formation of hydrazine is negligible. However, the fast $NH_2 + NH$ reaction (R9, R10) leads to formation of diazene. Marshall et al. [28] investigated the chemistry of the diazene isomers, emphasizing the relative importance of trans and cis configurations of HNNH. They calculated rate constants for the isomerization between tHNNH and cHNNH (R16), for thermal dissociation (R17, R18), and for the H-abstraction reactions to form NNH (R19, R21).

Compared to the very recent model by Alturaifi et al. [17], differences in specific rate constants are mostly minor and within the uncertainty of the value in the measured direction. However, as discussed above there are issues with the thermodynamic properties, particularly for NH_3 and NH, affecting the reverse rate constants for many reactions in the amine subset. Furthermore, the inclusion of an updated diazene subset, based on the recent work by Marshall et al. [28], has implications

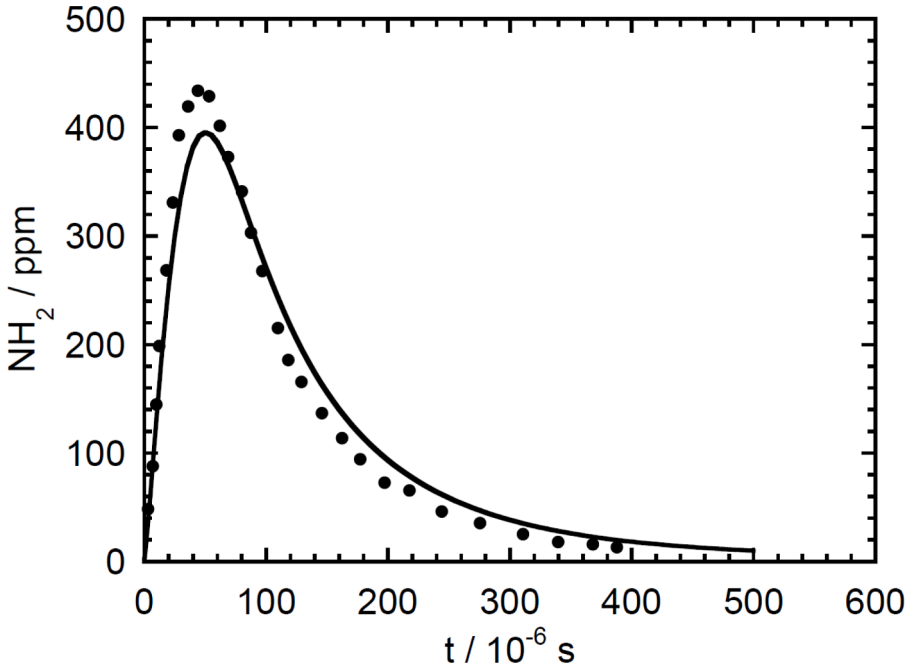

Fig. 10. Comparison of the shock tube measurements of NH_2 by Davidson et al. [15] with modeling predictions in decomposition of NH_3. Experimental conditions: 0.27% NH_3 in Ar at 0.902 atm and 2781 K.

for predictions at longer reaction times.

2. Results and discussion

Ammonia decomposition has been studied in batch reactors [21], flow reactors [18,19], jet-stirred reactors [20], and shock tubes [7–17]. There is a concern about data obtained in laboratory reactors, because they may be affected by reaction on the surface [6,17,62]. To avoid this uncertainty, only data from shock tube experiments are selected for modeling in the present work. However, also shock tube experiments are prone to uncertainties, typically caused by temperature or boundary effects at elevated reactant levels. Furthermore, the recent work of Alturaifi et al. [17] showed that even passivation methods used in shock tubes are not fully satisfactory when it comes to having the desired NH_3 initial concentration in a mixture. This uncertainty is a concern, particularly when the NH_3 concentration is not monitored directly.

The reported shock tube experiments can be divided into two groups, depending on the dilution level of the NH_3. First we look at results obtained at comparatively dilute conditions, i.e., with ammonia levels of 0.5% or below. Alturaifi et al. [17] monitored the NH_3 decay as a

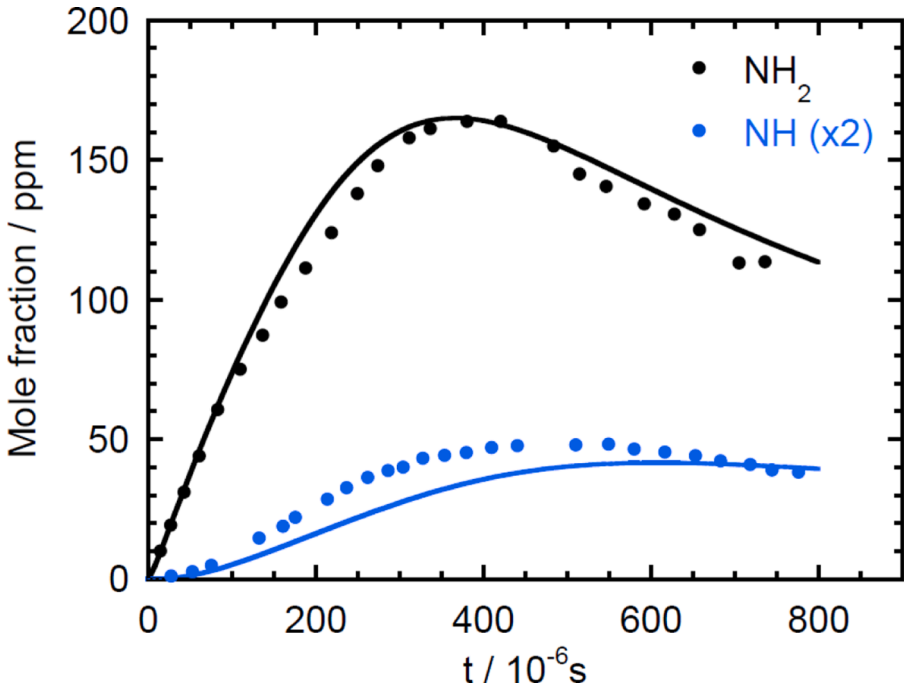

Fig. 11. Comparison of the shock tube measurements of NH_2 and NH by Davidson et al. [15] with modeling predictions in decomposition of NH_3 at about 2300 K. Experimental conditions: 0.27% NH_3 in Ar at 1.028 atm and 2301 K (for NH_2) and 0.3% NH_3 in Ar at 0.986 atm and 2294 K (for NH).

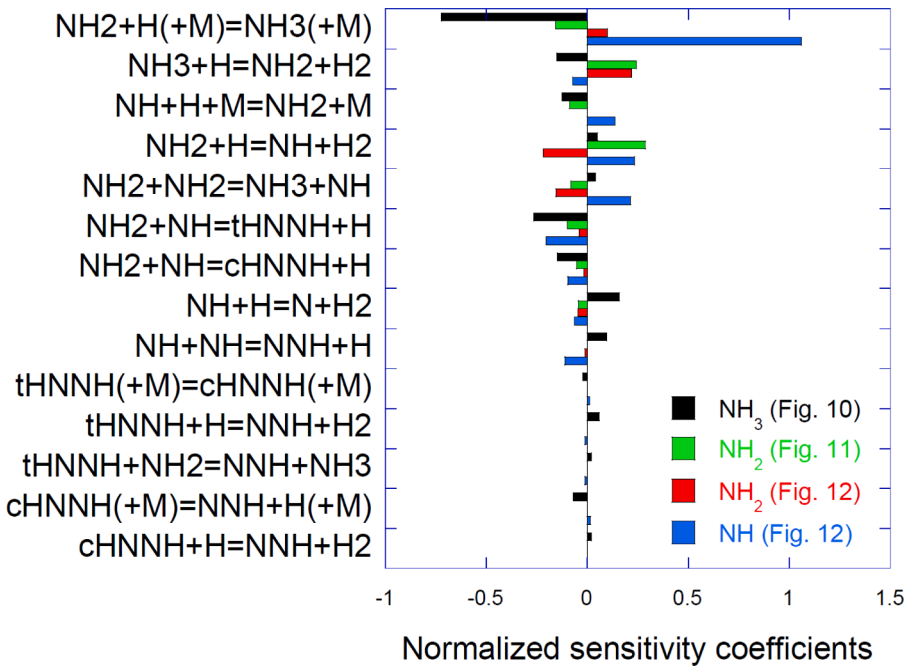

Fig. 12. Sensitivity coefficients for NH_3, NH_2 and NH for the conditions of Fig. 9 (2360 K, at 1000 μs), Fig. 10 (at 70 μs), Fig. 11 (at 400 μs for NH_2 and at 300 μs for NH).

function of time in shock tube experiments with initial concentrations of ammonia of about 0.5%. Figure 9 compares their measurements with modeling predictions for four temperatures in the range 2100-2500 K. The predictions are seen to capture the measurements quite well over the range investigated. The agreement in the initial stages lends support to the present value of the $NH_2 + H$ (+M) rate constant. At longer reaction times, the calculated NH_3 consumption rate is slightly too fast at the highest temperature, possibly due to uncertainties in secondary reactions, as discussed below.

Davidson et al. [15] detected NH_2 and NH profiles in NH_3 decomposition. Based on their measurements, they derived rate constants for reactions of NH_2 with H (R4), NH (R9, R10) and NH_2 (R5). Figure 10 compares their measured NH_2 profile with modeling predictions at 2781 K and close to atmospheric pressure.

In the initial stage, NH_2 is formed from dissociation of NH_3 (R1b). The good agreement with the observed early NH_2 gradient supports the value of $k_{1,0}$ in the model. Quickly a radical pool develops and NH_2 is then formed mainly by $NH_3 + H$ (R2). The location and value of the NH_2 peak is determined by the competition between formation through R2 and consumption by reactions with H (R4) and NH (R9), as well as by

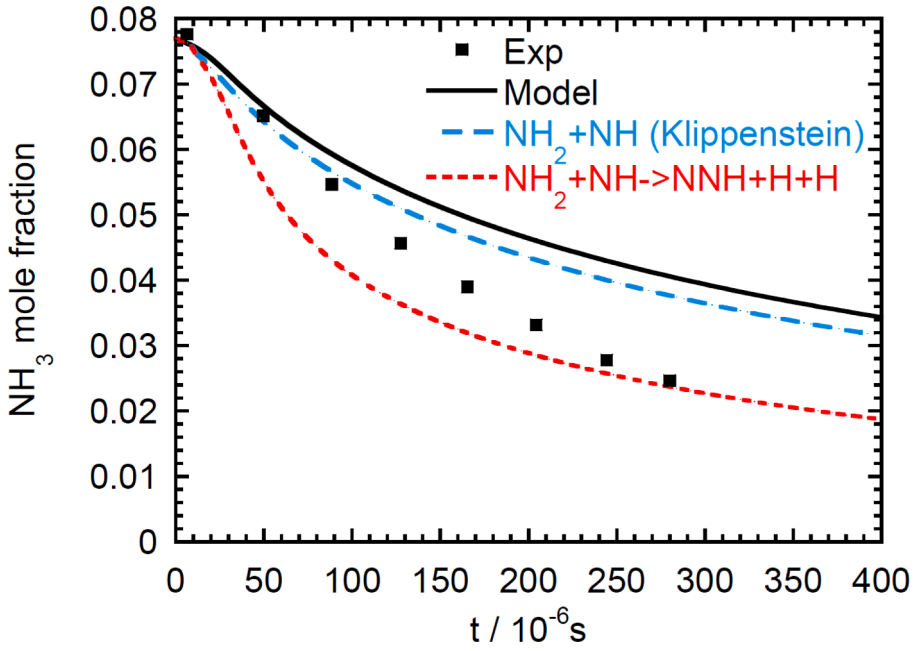

Fig. 13. Comparison of the shock tube measurements of NH_3 decay by Holzrichter and Wagner [14] with modeling predictions in decomposition of NH_3. Experimental conditions: 7.7% NH_3 in Ar at 3.94 atm and 2355 K. The dashed lines show modeling predictions showing the effect of changing the rate constant and products for the $NH_2 + NH$.

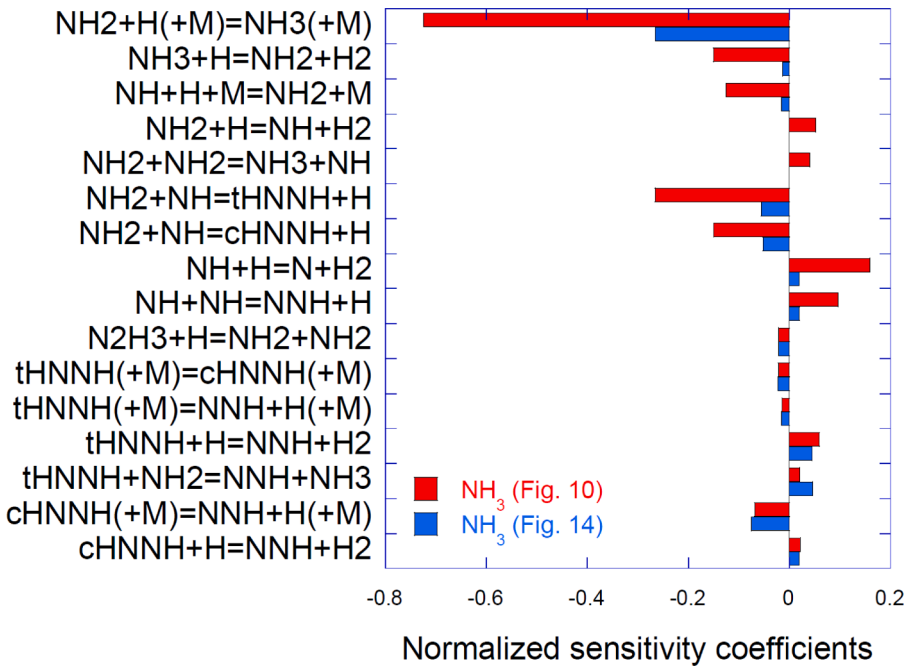

Fig. 14. Sensitivity coefficients for NH_3 for the conditions of Fig. 9 (0.5% NH_3, 2360 K, at 1000 μs) and Fig. 13 (7.7% NH_3, 2355 K, at after 200 μs).

thermal dissociation (R3b).

Figure 11 compares measured NH_2 and NH profile with modeling predictions at approximately 2300 K. Similar to the results at higher temperatures (Fig. 10), the NH_2 profile is captured well. Also the NH prediction is satisfactory, given the uncertainty in several of the key NH_2 and NH reactions in the mechanism.

A sensitivity analysis for the conditions of Figs. 9-11 was conducted; the results are shown in Fig. 12. The predicted NH_3 consumption rate under the conditions of Fig. 9 is primarily sensitive to its thermal dissociation (R1b) and the reaction with H (R2). However at longer times, formation of diazene through the $NH_2 + NH$ reaction (R9, R10) and the subsequent steps of HNNH has some impact on the NH_3 decay rate due to their influence on the radical pool. Also thermal dissociation of NH_2 (R3b) and NH + H (R14) turn up as sensitive.

The predicted NH_2 and NH profiles in Fig. 11 are sensitive mostly to reactions forming or consuming these radicals. The NH concentration appears to be slightly underpredicted at short times, while at longer times the consumption rate is underestimated. Early NH formation could be increased by increasing the rate constants for $NH_2 + M$ (R3b), $NH_2 +$ H (R4), and $NH_2 + NH_2$ (R5) or reducing the $NH_2 + NH$ (R9, R10) rate constant. All of these steps involve some uncertainty. However, changes made to improve the NH prediction would deteriorate the calculation of NH_2 (size and location of peak).

A number of the shock tube studies were conducted at elevated NH_3 reactant levels (6-8%) [7,11,14]. Jacobs [7] and Holzrichter and Wagner [14] monitored the NH_3 decay, while Dove and Nip [11] reported relative measurements of NH_2 and NH, together with absolute levels of N_2. Due to the high initial NH_3 concentrations, secondary reactions control the consumption rate at longer reaction times to a higher extent than for the more dilute experiments discussed above. However, the accuracy of the results obtained at lower dilution is in discussion due to concerns about thermal effects and boundary layer effects at longer reaction times. Furthermore, for the results reported by Jacobs [7] and by Dove and Nip [11] it proved difficult to capture the early observed reactivity (NH_3 consumption [7] or N_2 formation [11]) by the model, even though it should be dominated by the well-known rate constant for NH_3 dissociation (R1b). These differences possibly indicate issues with estimating the starting NH_3 concentration (Jacobs) or with sampling for mass spectrometric measurements (Dove and Nip).

The most reliable shock tube measurements conducted at elevated NH_3 levels are those reported by Holzrichter and Wagner [14], who investigated NH_3 decomposition over a fairly wide range of pressure and temperature. Figure 13 compares their only reported NH_3 concentration profile with modeling predictions. The calculations are in good agreement with the experiment at short times, where the NH_3 consumption is dominated by thermal dissociation. However, at longer times, predictions deviate from the experiment. Both the measured and calculated ammonia decomposition rates decrease after a while, but this effect is more pronounced in the modeling compared to the experimental observations. Modeling of the experiments by Jacobs [7], correcting the starting concentration NH_3 to match early data points, show deviations similar to those of Fig. 13; the NH_3 consumption rate is underpredicted at longer reaction times.

Figure 14 compares sensitivity coefficients for NH_3 at 50% conversion for dilute (0.5% NH_3, Fig. 9) and less dilute (7.7% NH_3, Fig. 13) conditions. As expected, the 0.5% NH_3 predictions are more sensitive to the reactions of NH_i species (NH_3, NH_2), while the 7.7% NH_3 calculations show a larger sensitivity to reactions in the diazene subset.

The overall reaction rate for the 7.7% NH_3 experiment is governed by the sequence,

$$NH_3 + H \rightleftarrows NH_2 + H_2 (R2)$$

$$NH_2 + H \rightleftarrows NH + H_2 (R4)$$

$$NH_2 + NH_2 \rightleftarrows NH_3 + NH (R5)$$

$$NH_2 + NH \rightleftarrows HNNH + H, (R9, R10)$$

followed by reactions of HNNH. Diazene, treated here as one species but in the model divided into the trans and cis isomers [28], either dissociates

$$HNNH(+M) \rightleftarrows NNH + H(+M), (R17, R18)$$

followed by rapid decomposition of NNH to form $N_2 + H$, or reacts with H (R19, R21) or NH_2 (R20, R22) in hydrogen abstraction steps. If dissociation (R17, R18) dominates over abstraction, the overall sequence is chain propagating; otherwise it is chain terminating. The observed discrepancy with experiment may be an indication that this

competition is not predicted accurately by the model.

To investigate this issue further, additional modeling predictions were conducted. First the impact of using the faster rate constant reported by Klippenstein et al. [24] for the $NH_2 + NH$ reaction (R9, R10) was investigated. This calculation, shown as a blue dashed line in Fig. 13, only shows a minor increase in the predicted NH_3 consumption rate. Then calculations assuming prompt dissociation of HNNH, corresponding to the $NH_2 + NH$ reaction yielding $NNH + H + H$ as products, was tested, shown in the figure as a red dashed line. This change has a significant impact on the predicted NH_3, showing the importance of reactions in the HNNH subset. This subset, which is based on calculated rate constants, has not yet been validated, since to our knowledge there are no experimental data available for pyrolysis of diazene.

Concluding remarks

The chemical kinetic model developed in the present work provides a satisfactory description of NH_3, NH_2, and NH concentration profiles reported from shock tube experiments on ammonia pyrolysis, at least under dilute conditions ($\leq$ 0.5% NH_3). For experiments conducted at higher NH_3 levels ($\approx$ 8%), the model apparently underpredicts the NH_3 consumption rate at longer times. The discrepancy may be caused by short-comings in the reaction mechanism. Several of the key steps in the ammonia pyrolysis mechanism are radical-radical reactions that are difficult to measure accurately and challenging to characterize theoretically. Furthermore, the diazene subset, which becomes important at longer times / higher reactant levels, has not been validated experimentally. However, the deviation could also be caused by experimental artifacts caused by the high reactant levels. There is a need for a comprehensive experimental characterization of ammonia pyrolysis to support further model development.

Declaration of Competing Interest

We declare no conflict of interest.

Acknowledgments

PG and HH would like to acknowledge funding from Innovation Fund Denmark for the AEngine Grand Solutions project. PM thanks the U.S. Department of Energy, Office of Basic Energy Sciences, Division of Chemical Sciences, Geosciences and Biosciences/Gas Phase Chemical Physics under Contract No. DESC0020952. Computational facilities were provided by the National Science Foundation, Grant CHE-1531468. The authors would like to thank Sulaiman Alturaifi and coworkers for sharing their manuscript on NH_3 pyrolysis prior to publication, along with measurement data in electronic form.

Supplementary material

Supplementary material associated with this article can be found, in the online version, at 10.1016/j.jfueco.2022.100049

References

[1] Hayakawa A, Goto T, Mimoto R, Arakawa Y, Kudo T, Kobayashi H. Laminar burning velocity and Markstein length of ammonia/air premixed flames at various pressures. Fuel 2015;159:98–106.
[2] Valera-Medina A, Xiao H, Owen-Jones M, David WIF, Bowen PJ. Ammonia for power. Prog Energy Combust Sci 2018;69:63–102.
[3] Kobayashi H, Hayakawa A, Somarathne KKA, Okafor EC. Science and technology of ammonia combustion. Proc Combust Inst 2019;37:109–33.
[4] Valera-Medina A, Amer-Hatem F, Azad A, Dedoussi I, Joannon MD, Fernandes R, Glarborg P, Hashemi H, He X, Mashurk S, McGowan J, Mounaim-Rouselle C, Ortiz-Prado A, Ortiz-Valera J, Rossetti I, Shu B, Yehia M, Xiao H, Costa M. A review on ammonia as a potential fuel: from synthesis to economics. Energy Fuels 2021;35:6964–7029.
[5] Glarborg P, Jensen A, Johnsson J. Fuel nitrogen conversion in solid fuel fired systems. Prog Energy Combust Sci 2003;29:89–113.
[6] Glarborg P, Miller J, Ruscic B, Klippenstein S. Modeling Nitrogen Chemistry in Combustion. Prog Energy Combust Sci 2018;67:31–68.
[7] Jacobs TA. Further shock-tube studies by infrared emission of the decomposition of ammonia. J Phys Chem 1963;67:665–7.
[8] Bradley JN, Butlin RN, Lewis D. Shock wave studies in nitrogen + hydrogen systems. Part 4. Thermal decomposition of ammonia. Trans Faraday Soc 1967;63:2962–9.
[9] Menon PG, Michel KW. Ultraviolet absorption of ammonia at high temperatures behind shock waves. J Phys Chem 1967;71:3280–4.
[10] Genich AP, Zhirnov AA, Manelis GB. Thermal Decomposition of Ammonia at Low and High Pressures in Shock Waves. Dokl Phys Chem 1973;212:897–900.
[11] Dove JE, Nip WS. A shock-tube study of ammonia pyrolysis. Can J Chem 1979;57:689–701.
[12] Yumura M, Asaba T, Matsumoto Y, Matsui H. Thermal decomposition of ammonia in shock waves. Int J Chem Kin 1980;12:439–50.
[13] Yumura M, Asaba T. Rate constants of chemical reactions in the high temperature pyrolysis of ammonia. Symp (Int) Combust 1981;18:863–72.
[14] Holzrichter K, Wagner HG. Thermal decomposition of ammonia behind shock waves. Symp(Int) Combust 1981;18:769–75.
[15] Davidson DF, Kohse-Höinghaus K, Chang AY, Hanson RK. A pyrolysis mechanism for ammonia. Int J Chem Kin 1990;22:513–35.
[16] Naumann C, Braun-Unkhoff M, Frank P. Thermal decomposition of ammonia behind shock waves. Proc 21st Symp Shock Tubes and Waves 1997;Paper 4260.
[17] Alturaifi SA, Mathieu O, Petersen EL. An experimental and modeling study of ammonia pyrolysis. Combust Flame 2022;235:116694.
[18] Monnery WD, Hawboldt KA, Pollock AE, Svrcek WY. Ammonia pyrolysis and oxidation in the Claus furnace. Ind Eng Chem Res 2001;40:144–51.
[19] Benes M, Pozo G, Abian M, Millera A, Bilbao R, Alzueta MU. Experimental Study of the Pyrolysis of NH_3 under Flow Reactor Conditions. Energy Fuels 2021;35:7193–200.
[20] Manna MV, Sabia P, Ragucci R, de Joannon M. Oxidation and pyrolysis of ammonia mixtures in model reactors. Fuel 2020;264:116768.
[21] Kim SH, Kim HS, Hwang JS, Choi JG, Chong PJ. In situ FTIR analysis for the thermal decompositions of trimethylgallium and trimethylgallium-ammonia adduct. Chem Mater 1994;6:278–81.
[22] Konnov AA, De Ruyck J. Kinetic modeling of the thermal decomposition of ammonia. Combust Sci Technol 2000;152:23–37.
[23] Bugler J, Somers KP, Simmie JM, Guthe F, Curran HJ. Modeling nitrogen species as pollutants: thermochemical influences. J Phys Chem A 2016;120:7192–7.
[24] Klippenstein SJ, Harding LB, Ruscic B, Sivaramakrishnan R, Srinivasan NK, Su M-C, Michael JV. Thermal decomposition of NH_2OH and subsequent reactions: Ab initio transition state theory and reflected shock tube experiments. J Phys Chem A 2009;113:10241–59.
[25] Li Y, Sarathy SM. Probing hydrogen–nitrogen chemistry: A theoretical study of important reactions in N_xH_y, HCN and HNCO oxidation. Int J Hydrogen Energy 2020;45:23624–37.
[26] Dievart P, Catoire L. Contributions of Experimental Data Obtained in Concentrated Mixtures to Kinetic Studies: Application to Monomethylhydrazine Pyrolysis. J Phys Chem A 2020;124:6214–36.
[27] Glarborg P, Hashemi H, Cheskis S, Jasper A. On the Rate Constant for NH_2+HO_2 and Third Body Collision Efficiencies for $NH_2+H(+M)$ and $NH_2+NH_2(+M)$. J Phys Chem A 2021;125:1505–16.
[28] Marshall P, Rawlins GR, Glarborg P. New reactions of diazene and related species for modeling combustion of amine fuels. Mol Phys 2021;in press. https://doi.org/10.1080/00268976.2021.1979674.
[29] Goos E., Burcat A., Ruscic B.. Ideal gas thermochemical database with updates from Active Thermochemical Tables. (<ftp://ftp.technion.ac.il/pub/supported/aetdd/thermodynamics> mirrored at <http://garfield.chem.elte.hu/burcat/burcat.html>; 2021.
[30] Feller D, Bross DH, Ruscic B. Enthalpy of formation of N_2H_4 (hydrazine) revisited. J Phys Chem A 2017;121:6187–98.
[31] Ruscic B, Bross D. Active Thermochemical Tables (ATcT), version 1.122p. (available at ATcT.anl.gov); accessed April 2021.
[32] Dorofeeva OV, Ryzhova ON, Suchkova TA. Enthalpies of formation of hydrazine and its derivatives. J Phys Chem A 2017;121:5361–70.
[33] Ko T, Marshall P, Fontijn A. Rate coefficients for the $H + NH_3$ reaction over a wide temperature range. J Phys Chem 1990;94:1401–4.
[34] Deppe J, Friedrichs G, Ibrahim A, Römming H-J, Wagner HG. The thermal decomposition of NH_2 and NH radicals. Ber Bunsenges Phys Chem 1998;102:1474–85.
[35] Whyte AR, Phillips LF. Products of reaction of nitrogen atoms with amidogen. J Phys Chem 1984;88:5670–3.
[36] Morley C. The mechanism of no formation from nitrogen compounds in hydrogen flames studied by laser fluorescence. Symp (Int) Combust 1981;18:23–32.
[37] Davidson DF, Hanson RK. High temperature reaction rate coefficients derived from N-atom ARAS measurements and excimer photolysis of NO. Int J Chem Kin 1990;22:843–61.
[38] Pagsberg PB, Eriksen J, Christensen HC. Pulse radiolysis of gaseous ammonia-oxygen mixtures. J Phys Chem 1979;83:582–90.
[39] Altinay G, Macdonald RG. Determination of the Rate Constants for the $NH_2(X^2B_1) + NH_2(X^2B_1)$ and $NH_2(X^2B_1) + H$ Recombination Reactions with Collision Partners CH_4, C_2H_6, CO_2, CF_4, and SF_6 at Low Pressures and 296 K. Part 2. J Phys Chem A 2012;116:2161–76.

[40] Altinay G, Macdonald RG. Determination of the rate constants for the $NH_2(X^2B_1)$ + $NH_2(X^2B_1)$ and $NH_2(X^2B_1)$ + H recombination reactions in N_2 as a function of temperature and pressure. J Phys Chem A 2015;119:7593–610.
[41] Baulch D, Bowman C, Cobos C, Cox R, Just T, Kerr J, Pilling M, Stocker D, Troe J, Tsang W, Walker R, Warnatz J. Evaluated kinetic data for combustion modeling: Supplement II. J Phys Chem Ref Data 2005;34:757–1397.
[42] Frisch MJ, Trucks G, Schlegel HB, Scuseria GE, Robb MA, Cheeseman JR, Scalmani G, Barone V, Petersson GA, Nakatsuji H, Li X, Caricato M, Marenich AV, Bloino J, Janesko BG, Gomperts R, Mennucci B, Hratchian HP, Ortiz JV, Izmaylov AF, Sonnenberg JL, Williams, Ding F, Lipparini F, Egidi F, Goings J, Peng B, Petrone A, Henderson T, Ranasinghe D, Zakrzewski VG, Gao J, Rega N, Zheng G, Liang W, Hada M, Ehara M, Toyota K, Fukuda R, Hasegawa J, Ishida M, Nakajima T, Honda Y, Kitao O, Nakai H, Vreven T, Throssell K, Jr JAM, Peralta JE, Ogliaro F, Bearpark MJ, Heyd JJ, Brothers EN, Kudin KN, Staroverov VN, Keith TA, Kobayashi R, Normand J, Raghavachari K, Rendell AP, Burant JC, Iyengar SS, Tomasi J, Cossi M, Millam JM, Klene M, Adamo C, Cammi R, Ochterski JW, Martin RL, Morokuma K, Farkas O, Foresman JB, Fox DJ. Gaussian 16 rev. a03. Wallington, CT, USA 2016.
[43] West NA, Millar TJ, Van de Sande M, Rutter E, Blitz MA, Decin L, Heard DE. Measurements of Low Temperature Rate Coefficients for the Reaction of CH with CH_2O and Application to Dark Cloud and AGB Stellar Wind Models. Astrophys J 2019;885:134.
[44] NIST Computational Chemistry Comparison and Benchmark Database. Number 101, Release 21. In: R. D. Johnson III, editor. NIST Standard Reference Database; October 2021.http://cccbdb.nist.gov/
[45] Troe J, Ushakov VG. The dissociation/recombination reaction CH_4 (+M) = CH_3 + H (+M): A case study for unimolecular rate theory. J Chem Phys 2012;136:214309.
[46] Dove JE, Nip WS. Shock tube studies of the reactions of hydrogen atoms. I. The reaction H + NH_3→ H_2 + NH_2. Can J Chem 1974;52:1171–80.
[47] Michael JV, Sutherland JW, Klemm RB. The flash photolysis-shock tube technique using atomic resonance absorption for kinetic studies at high temperatures. Int J Chem Kinet 1985;17:315–26.
[48] Michael JV, Sutherland JW, Klemm RB. Rate constant for the reaction, atomic hydrogen + ammonia, over the temperature range, 750-1777 K. J Phys Chem 1986;90:497–500.
[49] Marshall P, Fontijn A. An HTP kinetics study of the reaction between ground-state H atoms and NH_3 from 500 to 1140 K. J Chem Phys 1986;85:2637–43.
[50] Demissy M, Lesclaux R. Kinetics of hydrogen abstraction by amino radicals from alkanes in the gas phase. A flash photolysis-laser resonance absorption study. J Amer Chem Soc 1980;102:2897–902.
[51] Hack W, Rouveirolles P, Wagner HG. Direct measurements of the reactions NH_2 + H_2 = NH_3 + H at temperatures from 670 to 1000 K. J Phys Chem 1986;90: 2505–11.
[52] Friedrichs G, Wagner HG. Direct Measurements of the Reaction NH_2 + H_2→ NH_3 + H at Temperatures from 1360 to 2130 K. Z Phys Chem 2000;214:1151–60.
[53] Miller J, Bowman C. Mechanism and modeling of nitrogen chemistry in combustion. Prog Energy Combust Sci 1989;15:287–338.
[54] Hanson R, Salimian S. Combustion chemistry of nitrogen. In: W.C. Gardiner J, editor. Combustion chemistry. Springer-Verlag, New York; 1984.
[55] Bahng M-K, Macdonald RG. Determination of the Rate Constants for the Radical-Radical Reactions NH_2 + NH_2 and NH_2 + H at 293 K. J Phys Chem A 2009;113: 2415–23.
[56] Röhrig M, Wagner HG. The reactions of NH ($X^3\Sigma$-) with the water gas components CO_2, H_2O, and H_2. Symp (Int) Combust 1994;25:975–81.
[57] Fontijn A, Shamsuddin SM, Crammond D, Marshall P, Anderson WR. Kinetics of the NH reaction with H_2 and reassessment of HNO formation from NH + CO_2, H_2O. Combust Flame 2006;145:543–51.
[58] Linder DP, Duan X, Page M. Ab Initio Variational Transition State Theory Calculations for the H + NH_2 = H_2 + NH Hydrogen Abstraction Reaction on the Triplet Potential Energy Surface. J Phys Chem 1995;99:11458–63.
[59] Mackie JC, Bacskay GB. Quantum Chemical Study of the Mechanism of Reaction between NH ($X^3\Sigma$-) and H_2, H_2O, and CO_2 under Combustion Conditions. J Phys Chem A 2005;109:11967–74.
[60] Röhrig M, Römming H-J, Wagner HG. A direct measurement of the reaction NH_3 + NH → $2NH_2$. Ber Bunsenges Phys Chem 1994;98:1332–4.
[61] Dransfeld P, Hack W, Kurzke H, Temps F, Wagner HG. Direct studies of elementary reactions of NH_2-radicals in the gas phase. Symp (Int) Combust 1985;20:655–63.
[62] Glarborg P, Dam-Johansen K, Miller J, Kee R, Coltrin M. Modeling the Thermal $DeNO_x$ process in flow reactors. Surface effects and nitrous oxide formation. Int J Chem Kinet 1994;26:421–36.